Quantification of receptor tyrosine kinase transactivation through direct dimerization and surface density measurements in single cells

Jody L. Swift[a,1], Antoine G. Godin[b,1], Kim Doré[c], Laure Freland[c], Nathalie Bouchard[c], Chelsea Nimmo[a], Mikhail Sergeev[b], Yves De Koninck[c], Paul W. Wiseman[a,b], and Jean-Martin Beaulieu[c,2]

Departments of [a]Chemistry and [b]Physics, McGill University, Montreal, QC, Canada H3G 0B1; and [c]Department of Psychiatry and Neuroscience, Université Laval and Centre de Recherche Université Laval Robert-Giffard (CRULRG), Québec, QC, Canada G1R 2G3

Edited by Solomon H. Snyder, Johns Hopkins University School of Medicine, Baltimore, MD, and approved March 14, 2011 (received for review December 13, 2010)

Cell signaling involves dynamic changes in protein oligomerization leading to the formation of different signaling complexes and modulation of activity. Spatial intensity distribution analysis (SpIDA) is an image analysis method that can directly measure oligomerization and trafficking of endogenous proteins in single cells. Here, we show the use of SpIDA to quantify dimerization/activation and surface transport of receptor protein kinases—EGF receptor and TrkB—at early stages of their transactivation by several G protein-coupled receptors (GPCRs). Transactivation occurred on the same timescale and was directly limited by GPCR activation but independent of G-protein coupling types. Early receptor protein kinase transactivation and internalization were not interdependent for all receptor pairs tested, revealing heterogeneity between groups of GPCRs. SpIDA also detected transactivation of TrkB by dopamine receptors in intact neurons. By allowing for time and space resolved quantification of protein populations with heterogeneous oligomeric states, SpIDA provides a unique approach to undertake single cell multivariate quantification of signaling processes involving changes in protein interactions, trafficking, and activity.

high content analysis | oligomers | monoamine | *N*-acetyl cystein | brain-derived neurotrophic factor

Cell surface receptor signaling involves dynamic spatial and temporal changes in protein oligomeric states, resulting in an intricate choreography of protein–protein interactions balanced with changes in receptor trafficking. For instance, activation of receptor tyrosine kinases (RTKs) by their cognate ligands enhances receptor dimer formation, internalization, and recruitment of monomeric receptors to the cell surface (1). Furthermore, RTKs can also be transactivated by G protein-coupled receptors (GPCRs) under certain circumstances (2–4). However, little is known about the dynamic effects of transactivation on RTK dimerization and surface trafficking. Indeed, the majority of research directed to understanding transactivation has been limited to biochemical assays (2–4) and provides limited information on the dynamics and/or spatial localization of this process within specific regions/compartments of cells/tissue.

Understanding receptor dynamics requires methods that can be applied to cells or tissue under physiologically relevant, nonsteady state conditions. Spatial intensity distribution analysis (SpIDA) is a method based on the fitting of fluorescence intensity histograms calculated from conventional laser-scanning confocal images to monitor protein oligomerization in live or fixed cells and tissues (5). By directly monitoring early interactions between endogenous proteins in single cells rather than relying on the detection of downstream signaling molecules, SpIDA potentially offers several advantages over conventional assays used to study cell surface receptor distributions (5). We apply SpIDA and compare it with fluorescence lifetime imaging microscopy (FLIM) to extract information about the transactivation by different GPCRs of two RTKs—the EGF receptor (EGFR) in Chinese hamster ovary (CHO-k1) cells and the brain-derived neurotrophic factor (BDNF) receptor TrkB in nontransfected/intact neurons.

Our results indicate that SpIDA allows for the quantitative pharmacological characterization of RTK transactivation and provides direct evidence for dynamic changes in RTK dimerization and trafficking in response to GPCR activation. Specifically, we show that, for all RTK-GPCR pairs investigated, RTK dimerization from GPCR stimulation occurs on the same timescale as direct stimulation. However, EGFR activation by GPCRs does not always result in the same level of internalization. In addition, the quantitative nature of SpIDA allows characterization of RTK transactivation using standard pharmacodynamic parameters, thereby providing a universal method for comparing studies between cell lines and receptor systems. Most importantly, SpIDA also detects cell-signaling mechanisms involving endogenous proteins in neurons, allowing for the monitoring of biological processes occurring in single cells directly in their native environment.

Results

Use of SpIDA to Detect and Quantify RTK Dimerization. CHO-k1 cells expressing GFP-tagged EGFR (EGFR-GFP) in absence of endogenous EGFR were used to establish the usefulness of SpIDA in measuring RTK dimerization in vivo. Western blot analysis validated the functionality of EGFR-GFP in this system. As expected, stimulation of these cells with EGF yielded increased phosphorylation of EGFR-GFP and its downstream targets Akt and extracellular-regulated kinase (Erk), which could be reversed by the use of tyrosine kinase inhibitor AG1478 (Fig. 1*A*). To determine conditions under which EGF induces EGFR dimerization, we used FLIM to measure Förster resonance energy transfer (FRET) in living cells. In these experiments, cells expressing EGFR-GFP (the FRET donor) were transfected with an additional EGFR-mCherry (the FRET acceptor) expression vector. The fluorescence lifetime of the GFP tag was measured under basal conditions or after 1-min stimulation with EGF at different doses (Fig. 1*B*). Calculated FRET efficiencies showed

Author contributions: J.L.S., A.G.G., K.D., L.F., Y.D.K., P.W.W., and J.-M.B. designed research; J.L.S., A.G.G., K.D., L.F., N.B., C.N., M.S., and J.-M.B. performed research; P.W.W. and J.-M.B. contributed new reagents/analytic tools; J.L.S., A.G.G., K.D., L.F., N.B., C.N., M.S., and J.-M.B. analyzed data; and J.L.S., A.G.G., Y.D.K., P.W.W., and J.-M.B. wrote the paper.

The authors declare no conflict of interest.

This article is a PNAS Direct Submission.

Freely available online through the PNAS open access option.

[1]J.L.S. and A.G.G. contributed equally to this work.

[2]To whom correspondence should be addressed. E-mail: martin.beaulieu@crulrg.ulaval.ca.

This article contains supporting information online at www.pnas.org/lookup/suppl/doi:10.1073/pnas.1018280108/-/DCSupplemental.

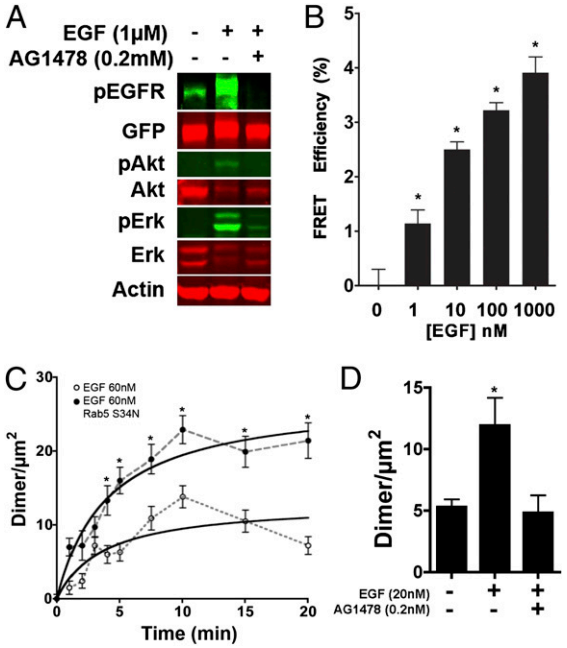

Fig. 1. SpIDA allows the detection and quantification of EGFR in cells. (*A*) Representative Western blot showing EGF-induced phosphorylation of EGFR (Tyr1068), Akt (Ser473), and ERK1/2 (Thr202/Tyr204) in response to EGF with or without preincubation with the tyrosine kinase inhibitor AG1478 in EGFR-GFP CHO-k1 cells. For each phosphoprotein, the corresponding total protein was detected on the same membrane using primary antibodies and combinations of secondary antibodies labeled with different fluorescent dyes (IR-Dye 800 in green and IR-Dye-700 in red). (*B*) Detection of EGF-induced EGFR dimerization by FLIM/FRET in CHO-k1 cells coexpressing EGFR-GFP and EGFR-mCherry. Data are presented as percentage of FRET efficiency compared with basal signal obtained from nonstimulated cells (n = 42–70 cells from three independent experiments per conditions). (*C*) SpIDA analysis of EGFR dimer density over time after stimulation with EGF (60 nM) without (n = 25 cells/point) or with Rab5 S34N (n = 25 cells/point). Both datasets are from a single fixed cell experiment. (*D*) SpIDA analysis of EGFR dimer density at 5 min after stimulation with EGF (20 nM) with or without AG1478 (0.2 mM; n = 10, 5, and 8 cells/bar, respectively). Data are means ± SEM. *$P \leq 0.05$ compared with unstimulated conditions (Mann–Whitney test).

a progressive increase of FRET with respect to ligand concentration, indicative of an increase in EGFR interaction. The increased FRET efficiency was detected at EGF concentrations as low as 1 nM (Fig. 1*B*), showing that measurements of EGFR interactions provide an index of activation.

We applied SpIDA and measured an increase in EGFR dimer density at the basal membrane as a function of time. The quantal brightness (ε) of monomeric GFPs, ε_0, was independently measured using a vector expressing a membrane-targeted monomeric GFP (5). No difference in ε was detected between images of mGFP and the ones of EGFR-GFP in serum-starved unstimulated cells, indicating that the vast majority (~90%) of the EGFRs were in a monomeric state before stimulation. Because EGF ligand-activated EGFR-GFP expressed alone did not exhibit any change in lifetime (as observed with FLIM) compared with nonstimulated cells, we concluded that the two fluorophores in the EGFR homodimer do not undergo any significant self-quenching. It is, hence, reasonable to estimate the ε of the EGFR-GFP dimers to be two times the monomeric brightness ($2\varepsilon_0$), thus allowing SpIDA to reliably measure interaction with a single fluorescent probe.

Using SpIDA, a logarithmic increase in EGFR-GFP dimer density was measured at the cell membrane as a function of time after stimulation with EGF (Fig. 1*C*). Interestingly, the dimer density seemed to decrease after 10 min (Fig. 1*C*). To assess whether this decrease was because of receptor internalization, we repeated the same experiment in cells co-transfected with a dominant negative Rab5 S34N mutant (Fig. 1*C*), which prevents EGFR endocytosis (6). In the Rab5 S34N mutant (+) cells, there was an overall reduction in large-scale clustering of the activated receptors occurring at times >10 min poststimulation (Fig. S1). We also noted a higher dimer density that became statistically significant at times >4 min. This reveals that dimer measurements with SpIDA were not an artifact of clustering but resulted from real dimerization of EGFRs. In agreement with Western blots (Fig. 1*A*), pretreatment of the cells with 0.2 nM AG1478 prevented the increase in dimer density in response to EGF (20 nM and 5 min) (Fig. 1*D*). These results show that, in agreement with FLIM/FRET measurements, SpIDA detects an increase in density of EGFR dimers at early times (<5 min), even when visual inspection of the images would suggest that no change in receptor distribution has occurred. Thus, measurement of RTK dimerization can also function as an index of receptor activation in single cells. In addition, the data illustrate that SpIDA provides quantitative information about both oligomerization and internalization.

SpIDA Detects EGFR Transactivation by GPCRs. We then applied EGFR dimer density measurements to determine whether it was possible to quantify the transactivation of RTKs by GPCR stimulation. EGFR-GFP–expressing cells were transfected with different GPCRs. Visual inspection of EGFR clustering in response to stimulation by different GPCRs suggests that, in contrast with direct EGFR stimulation, activation of some GPCRs did not result in observable large-scale clustering of EGFR (Fig. S2). Stimulation of the Angiotensin 1a receptor (At1aR) with Angiotensin II (AngII) and activation of the β_2-adrenergic receptor (β_2AR) with Isoproteranol (Iso) did not cause visible changes in EGFR distribution, whereas noticeable changes were observed for cells expressing the dopamine 2 receptor (D2R) stimulated with apomorphine (Apo). However, transactivation of EGFR has been reported for both At1aR and β_2AR (2, 3). Furthermore, both FLIM/FRET and SpIDA analyses indicate that At1aR is capable of inducing EGFR dimerization (Fig. 2 *A* and *B*).

To generate temporal transactivation/EGFR dimerization profiles, we applied SpIDA to cells cotransfected with At1aR and stimulated with AngII (Fig. 2*B*). To establish that increased EGFR-GFP dimer density corresponds to transactivation, these experiments were repeated in presence of *N*-acetyl cysteine (NAC), which has been shown to inhibit RTK transactivation but not affect activation by EGF (7). NAC completely inhibited the increase in EGFR dimer density (Fig. 2*B*) observed for AngII stimulation without preventing normal EGF-induced dimerization (Fig. 2*C*). Finally, control measurements were performed using cells expressing EGFR without any additional GPCR and were stimulated with AngII, Apo, and Iso. In none of these cases was a rise in dimer density observed (Fig. 2*D*). We conclude that the increase in EGFR dimerization detected by SpIDA in response to these compounds results from the stimulation of the transfected GPCRs and thus, represents RTK-GPCR transactivation. In total, these results show that measurement of RTK dimerization can also be used as an index for transactivation.

Combined Measurements of Dimerization and Internalization with SpIDA. Receptor activation is generally considered to occur in equilibrium with internalization, desensitization, and recycling. However, our observations suggest that transactivation and internalization may be regulated differentially. To examine the relationship between transactivation and internalization, a technique is needed that can provide quantitative information concomitantly on oligomerization and total surface receptor density in single cells, and it must be able to resolve both activated and nonactivated receptors. FRET-based techniques do not provide easy access to quantitative information on the noninteracting fluorescent species. Moreover, homo-FRET often requires a

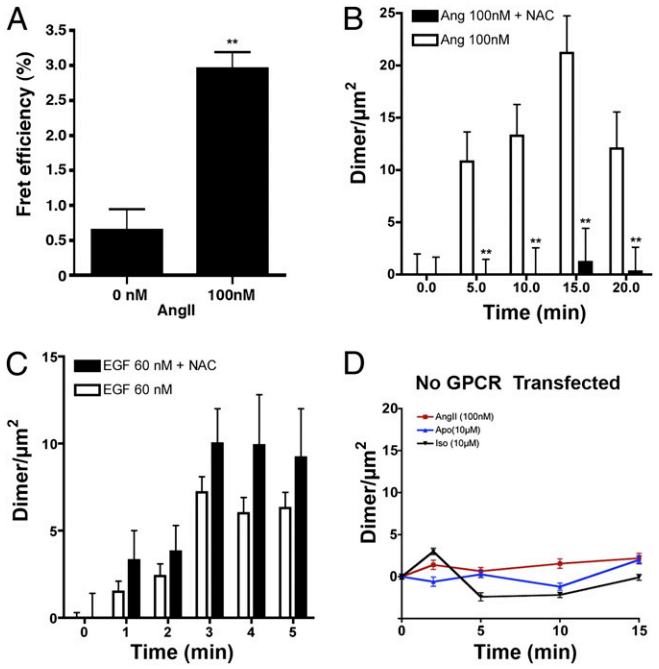

Fig. 2. Dimerization and endocytosis of EGFR in response to GPCR stimulation as detected by SpIDA. (*A*) Detection by FLIM/FRET of EGFR dimerization 1 min after stimulation with AngII (100 nM) in CHO-k1 cells coexpressing EGFR-GFP, EGFR-mCherry, and At1aR receptors. Data are presented as percentage of FRET efficiency compared with basal signal obtained from nonstimulated cells (n = 42–70 cells from three independent experiments per condition). (*B*) Effect of the transactivation inhibitor NAC on EGFR dimer density measured by SpIDA over time after stimulation with AngII (100 nM) in CHO-k1 cells coexpressing EGFR-GFP At1aR receptors in the presence (n = 4 cells/point) and absence of NAC (n = 17 cells/point). Both curves were obtained from a single live cell assay. (*C*) Comparison of EGFR dimerization under direct stimulation with 60 nM EGF in the presence (n = 25 cells/bar) and absence of NAC (n = 14 cells/bar). Both curves have the same temporal profile within error. (*D*) SpIDA detects no increase in dimer density in response to GPCR ligands Ang (100 nM) or Iso (10 μM) or the selective dopamine receptor agonist Apo (10 μM) in CHO-k1 cells expressing EGFR-GFP without additional GPCRs (n = 28 cells/point for all points). All data are means ± SEM. $^{**}P \leq 0.01$ (Mann–Whitney test) compared with unstimulated conditions (*A*) or NAC-treated condition at the same time point (*B*).

specialized anisotropy imaging setup and estimation of the anisotropy after energy transfer, which is not trivial to predict (8). In contrast, SpIDA easily allows the direct measurements of oligomeric mixtures, even in heterogeneous sample populations, and it is not subject to some of the potential biases of FRET (e.g., increased probability of collisional FRET). Thus, SpIDA was the ideal choice for the remainder of the measurements.

We further examined the relationship between transactivation and internalization in a dose-dependent manner for a number of EGFR-GPCR pairs, including At1aR, β_2AR, D2R, dopamine 1 receptor (D1R), and neurokinin 1 receptor (NK-1r). From the temporal transactivation profile (Fig. 2*B*), we established that, like direct activation, transactivation results in very rapid EGFR dimer formation. Thus, for the remainder of the experiments, all measurements were done at 1 min poststimulation. Presented in Fig. S3 are the monomer, dimer, and total protein densities measured for EGFR cells expressing β_2AR and D2R, illustrating a case where transactivation does not result in rapid endocytosis (Fig. S3 *A–C*) and a case in which EGFR is internalized rapidly (Fig. S3 *D–F*) on transactivation, respectively.

For the transactivation of EGFR through β_2AR activation, we observe a decrease in the monomer density (Fig. S3*A*) and a corresponding increase in dimer density (Figs. S3*B* and S4) with increased concentration of agonist. Additionally, we note a small overall increase in total EGFR density (Figs. S3*C* and S4) at high ligand concentrations (100 μM), suggesting limited internalization of activated EGFR dimers at 1 min and possible recruitment of new EGFR. Furthermore, stimulation of β2AR with 10 μM Iso did not affect the surface expression of EGFR measured at later time points (Fig. S3*G*). Similar results were obtained for transactivation of EGFR by stimulation of At1aR with AngII (tabulated in Fig. S3*H*).

Very different results were obtained for EGFR-D2R transactivation carried out in absence of the Rab5 S34N mutant. Measured dimer densities for high concentrations of ligand (>60 μM) were lower than the basal level of dimers (Fig. S3*E*). We observed a corresponding decrease in both monomer (Fig. 3*D*) and total particle density (Fig. S3*F*) for 60 μM Apo and a slight recovery for 80 μM Apo. This recovery in dimer density was attributed to recruitment of new EGFR to the cell surface based on the observed increase in monomeric EGFR density. The addition of the Rab5 S34N mutant prevented endocytosis of the activated EGFR dimers (Fig. S3*E*) and provided a stabilization of total protein concentration at the membrane (Fig. S3*F*). Similar results were obtained for transactivation of EGFR-GFP with D1R and NK-1r (Fig. S3*H*). Taken together, these results indicate that transactivation and internalization are not necessarily interdependent. In fact, there seems to be no correlation between the maximum degree of transactivation achieved and the ability for a GPCR to induce rapid internalization of EGFR.

Pharmacological Quantification of EGFR Transactivation. Using SpIDA, we generated concentration response curves of measured dimer density vs. ligand concentration for both direct stimulation (Fig. 3*A*) and transactivation of EGFR by five different GPCRs (Fig. 3 *B–G*). For each of the concentration response plots, the initial dimer density (basal) was subtracted from the subsequent values to compare data from independent experiments. The curves were fit using the Hill Langmuir binding isotherm model to obtain two pharmacologically relevant values: D_{50} (concentration required to obtain 50% maximum EGFR dimer density signal) and D_{max} (maximal level of EGFR dimer density signal) for each ligand-GPCR pair (Fig. 3 and Table S1). It is noteworthy that the fitted D_{50} values are consistent overall with both the $FRET_{50}$ values obtained (concentration required to achieve 50% FRET efficiency) and published range of K_d values (Table S1). We also compared the effects of two different naturally occurring peptidic ligands for NK-1r on EGFR dimerization (Fig. 3 *F* and *G*). Importantly, the curve for neurokinin A (NKA) (Fig. 3*F*), the lower-affinity ligand, is shifted to the right compared with the curve for substance P (Fig. 3*G*), the higher-affinity ligand, and this is reflected in the measured D_{50} values.

Comparison of the EGFR dimerization curves under direct stimulation (Fig. 3*A*) to concentration response curves occurring from transactivation suggests that, for all cases of transactivation, the full D_{max} was not achieved. To determine if the amount of transfected GPCR was the limiting factor in the maximum achievable dimerization signal, we carried out an experiment where we compared the concentration response curves for the same receptor (NK-1r) with increased GPCR concentration (Fig. 3*H*). Under these conditions, we noted that, by quadrupling the number of transfected receptors, an increase in D_{max} but not in D_{50} was observed. Similar effects were also obtained by varying β_2AR-transfected receptor levels in a separate set of experiments (Table S1). This shows that the potency of EGFR transactivation is defined by the activation of the GPCR by its ligand, whereas maximum transactivation levels are limited by GPCR expression.

Finally, compilation of the different concentration response curves indicate that transactivation of RTK by GPCRs is not limited to a single class of GPCR but can occur for both class A (β_2AR, D1R, and D2R) and class B (At1aR and NK-1r) GPCRs. Furthermore, GPCRs coupling to different G proteins ($G\alpha_q$: NK-1r and AT1aR; $G\alpha_{i/o}$: D2R;

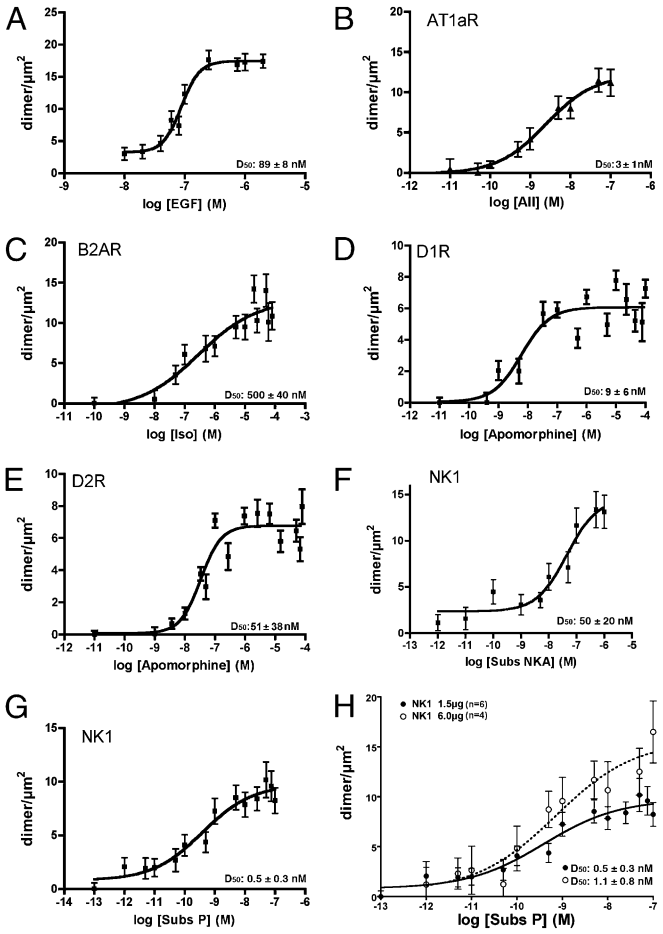

Fig. 3. SpIDA allows the pharmacological characterization of EGFR transactivation by diverse GPCRs. (*A*) Dose-response curves of EGFR dimer density 1 min after direct stimulation by EGF in CHO-k1 cells (n = 111 cells/point from six individual titrations). (*B–G*) Dose-response curves of EGFR dimer density response 1 min after stimulation of GPCRs by (*B*) AngII (n = 125 cells/point), (*C*) Iso (n = 107 cells/point), (*D* and *E*) Apo (n = 322 cells/point for D2R and n = 260 cells/point for D1R, respectively), (*F*) SubsP (n = 120 cells/point), and (*G*) NKA (n = 134 cells/point) in CHO-k1 cells cotransfected with Rab5 S34N for either (*B*) At1aR, (*C*) B2AR, (*D*) D2R, (*E*) D1R, or (*F* and *G*) NK-1r (generated using six individual titrations). (*H*) Dose-response curves of EGFR dimer density 1 min poststimulation of either 1.5 (n = 120 cells/point from six individual titrations) or 6 μg (n = 60 cells/point from three individual titrations) of NK-1r by SubsP in CHO-k1 cells co-transfected with Rab5 S34N. Data are means ± SEM.

$G\alpha_s$: D1R and β_2AR) were all able to induce EGFR dimerization in a dose-dependent manner. This suggests that GPCRs may regulate RTKs activation and internalization through a number of different second messenger pathways or may involve shared G protein-independent signaling mechanisms (9). More importantly, these results show that SpIDA is suitable for generating quantitative concentration response curves in single cells for EGFR transactivation with high sensitivity.

Transactivation of Endogenous TrkB by Endogenous Dopamine Receptors in Neurons. We used striatal neuron cultures to establish whether SpIDA can be used to measure the transactivation of endogenous TrkB by endogenous GPCRs (D1R or D2R). Primary striatal neuron cultures mainly express either D1Rs or D2Rs. To differentiate between these neuronal subtypes, cultures were prepared from 3-d-old double BAC transgenic mice expressing GFP under the control of the D2R gene promoter and the dt-tomato fluorescent protein under the control of the D1R gene promoter (10). As shown in Fig. 4*A*, most cells expressed either the D1R or D2R and were mostly segregated into two subpopulations of neurons in culture, which is the case in the adult mouse striatum (11).

Neurons were treated with either the TrkB ligand BDNF or a D1R/D2R agonist. Surface-expressed endogenous TrkB was detected by standard immunofluorescence (Fig. 4 *B* and *C*). Cells treated with the tyrosine kinase inhibitor AG1478 were used to estimate monomeric TrkB ε for each separate set of experiments. As shown in Fig. 4 *D* and *E*, stimulation with BDNF resulted in increased TrkB dimerization and reduced surface expression. Similarly, stimulation with Apo increased dimerization of endogenous TrkB in neurons expressing either D1R or D2R (Fig. 4*F*), thus indicating that endogenous dopamine receptors can transactivate endogenous TrkB, at least in striatal neurons, and that SpIDA can be used to detect this process. The ability of both types of dopamine receptors, each coupled to different G proteins, to cause transactivation under native conditions shows that this phenomenon is not limited to recombinant systems or GPCR coupled to the same G protein. Finally, both direct activation of TrkB and transactivation in D1R-expressing neurons resulted in a reduction in total surface protein density consistent with receptor internalization, whereas the tyrosine kinase inhibitor AG1478 increased RTK surface expression in D1R- and D2R-expressing neurons as it did in CHO-k1 cells (Fig. 4 *E* and *G*). SpIDA, thus, allowed us to perform quantitative analysis of both RTK transactivation and trafficking in single native cells.

Discussion

Rapid and localized changes in protein–protein interactions leading to the formation of oligomeric protein complexes are of central importance for cell signaling. To understand the fine regulation of signaling in vivo, it is essential to develop tools that are able to quantify interactions of endogenous cellular proteins in a time- and space-resolved fashion at the single-cell level. Here, we used the specific case of RTK transactivation by GPCRs to show the usefulness of SpIDA to achieve this goal. We have successfully used SpIDA to quantify EGFR dimerization and surface shuttling in response to stimulation of five different GPCRs (At1aR, β_2AR, D1, D2R, and NK-1r) in transfected cells and have detected endogenous TrkB dimerization and internalization after endogenous dopamine receptor (D1R or D2R) stimulation in neurons. This validates SpIDA as a suitable tool for the quantitative analysis of cell surface oligomerization events associated with changes in activity in single cells for both transfected systems and endogenous expression.

SpIDA is compatible with antibody detection to obtain oligomerization data for endogenous cellular proteins (5) and presents substantial advantages over FRET and other imaging techniques used to study RTK-GPCR transactivation. We showed that both FRET and SpIDA are capable of measuring an increase in EGFR dimerization in response to GPCR stimulation in transfected cells. In addition, SpIDA is also suitable for single-color analysis, requiring only one type of fluorescent label, and it allows for measurements of proteins at native levels for which fluorescent probes exist (specific antibodies or fluorescent proteins). Furthermore, SpIDA can detect indirect protein–protein interactions within common assemblies, even in absence of energy transfer (e.g., in the presence of a third partner that increases the distance between the donor– acceptor pair). Finally, by monitoring both dimer density and total particle density, SpIDA allows one to obtain more information about processes within the cell (i.e., internalization and recruitment of more receptors to the cell surface). In contrast to SpIDA, techniques based on temporal fluctuations used to measure concentration and oligomerization states [e.g., fluorescence correlation spectroscopy (FCS) (12), fluorescence intensity distribution analysis (FIDA) (13), and photon-counting histogram (PCH) (14)] do not give reliable

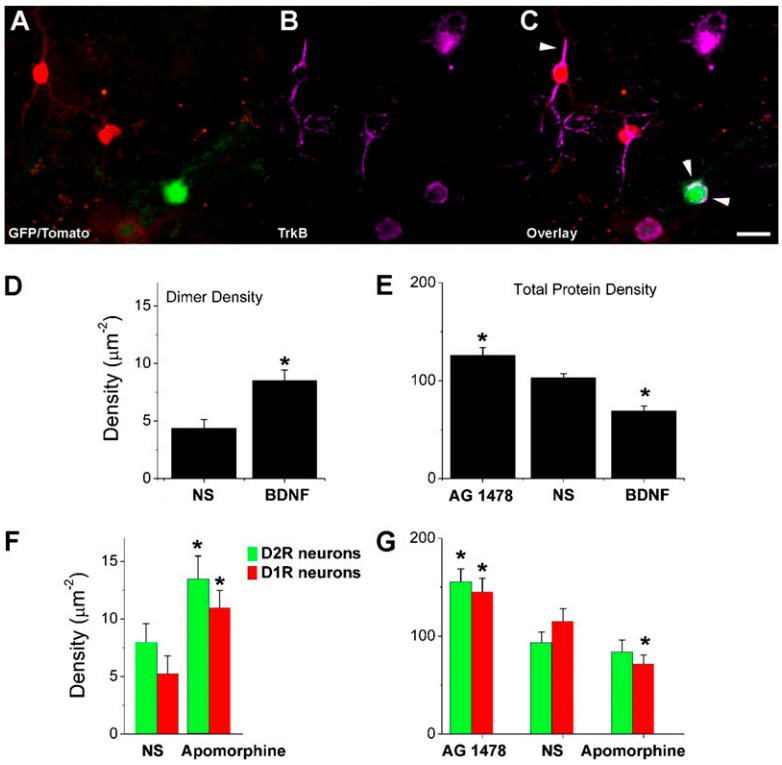

Fig. 4. SpIDA allows for the detection and quantification of endogenous TrkB activation by endogenous dopamine receptors in striatal neurons. (*A–C*) Surface immunodetection of endogenous TrkB in striatal neurons prepared from BAC transgenic mice expressing a GFP (green) reporter gene in cells having endogenous D2R or a tomato (red) reporter gene in cells having endogenous D1R. Arrowheads in *C* indicate surface TrkB labeling on striatal neurons expressing different dopamine receptors. (Scale bar, 15 μm.) (*D* and *E*) SpIDA analysis of TrkB dimer (*D*) and surface densities (*E*) of neurons after incubation with AG1478 (0.2 mM for 30 min at 37 °C; n = 31 neurons) under nonstimulated condition (n = 93 neurons) and after direct stimulation with BDNF (50 pM for 3 min at 37 °C; n = 83 neurons). (*F* and *G*) SpIDA analysis of TrkB dimer (*F*) and surface densities (*G*) of neurons after incubation with AG1478 (0.2 mM for 30 min at 37 °C; D2R n = 30 neurons and D1R n = 33 neurons) under nonstimulated condition (D2R n = 19 neurons and D1R n = 26 neurons) and after stimulation of endogenous dopamine receptors with apomorphine (2 μM for 3 min at 37 °C; D2R n = 33 neurons and D1R n = 38 neurons). Data are presented for subpopulations of striatal neurons expressing D1R or D2R. All data are means ± SEM. *$P \leq 0.05$ (Mann–Whitney test).

results on density at the membrane in biological systems undergoing rapid dynamic changes. By definition, these techniques require that the density of the system and the oligomerization state of the targeted proteins stay constant during the whole experiment (~100 s because of the slow diffusion of RTKs at the membrane) (15). In RTK activation or transactivation, substantial changes in oligomerization states occur within the first few minutes after stimulation, and SpIDA, which is applied to single images, is useful for capturing and quantifying these processes.

SpIDA provides quantitative data on the dynamics of cell surface receptor transitions from monomeric to dimeric states at the single cell level. Using dimerization as an index of activation, we measured concentration response curves, allowing us to calculate both D_{50} and D_{max} values to compare and evaluate RTK activation occurring in response to direct stimulation or indirect GPCR stimulation. The measured D_{50} values for EGFR direct stimulation as well as the $FRET_{50}$ value obtained under comparable conditions were similar and slightly higher than published K_d values for EGF-EGFR binding interaction (Fig. 3 and Table S1). Under our experimental conditions, we start with a small population of preformed dimers (Fig. S3*H*) and a large population of monomeric EGFR. It is believed that preformed dimers account for high-affinity binding of EGF to EGFR, and monomeric ligand-induced dimerization accounts for a population of receptors with lower-affinity binding (16, 17). Both SpIDA and FLIM/FRET measure the response (dimerization) of the low-affinity population. It is, thus, expected that the D_{50} and $FRET_{50}$ values should be slightly lower than the reported K_d value given the high-affinity population.

Most studies of RTK transactivation (4, 18, 19) focused mostly on specific RTK/GPCR pairs, and the methods used to study these pairs did not allow for the comparison of similarities and differences in the dynamics of RTK transactivation by different GPCRs. In contrast, the ease of application of SpIDA to large datasets allowed us to examine the activation of EGFR by five GPCRs, three class A (β_2AR, D1R, and D2R) and two class B (At1aR and NK-1r) (20). The examination of D_{50} values obtained for the EGFR/GPCR transactivation pairs indicates that the experimental values obtained using SpIDA all fall within the range of K_d values reported in the literature. These observations were further supported by $FRET_{50}$ values obtained in separate transactivation experiments involving At1aR receptors. In contrast, D_{max} values obtained for transactivation experiments were lower than those obtained after direct stimulation and were limited by GPCR expression level (Fig. 3). Based on these findings, we conclude that, in most cases, the transactivation of EGFR happens rapidly after GPCR activation and may be closely related to the binding kinetics of these receptors by their respective agonists.

Prolonged stimulation (30 min) of β_2AR induces some level of EGFR internalization detectable by biochemical methods in transfected cells, a phenomenon that has been associated with proposed mechanisms for transactivation (2, 21). However, direct measurement of surface monomer, dimer, and total particle densities at early time points indicates that not all GPCRs are equal in their ability to induce the internalization of EGFR (Fig. S3). D1R, D2R, and NK-1r receptors induced rapid EGFR internalization and required the addition of the Rab5 S34N mutant to obtain full concentration response curves. In contrast, At1aR and β_2AR did not cause rapid EGFR internalization while inducing the formation of EGFR dimers through transactivation (Fig. S3 and Fig. 3). Therefore, direct quantification at early stages of the transactivation process (1 min) shows that internalization is not necessary for EGFR dimerization and that it does not occur rapidly. Furthermore, because Rab5 S34N can also prevent full GPCR internalization (22), observation of RTK transactivation in cells expressing this mutant suggests that full GPCR internalization may not be required for RTK transactivation. Differences in the induction of EGFR internalization also provide a way to classify RTK-GPCR transactivation pairs by their ability to induce rapid endocytosis of the RTKs. Because RTKs are believed to be capable of signaling on endocytic vesicles (4), the differential ability of GPCRs to induce rapid internalization of transactivated RTK may also have functional consequences in vivo.

Most research conducted on RTK transactivation by GPCRs has been performed in overexpression recombinant cell systems, and few studies have addressed the relevance of these biochemical phenomena across cell types or in native conditions. Previous studies have shown that two G_α-coupled GPCRs, the Adenosine A2a and the pituitary adenylate cyclase activating peptide receptors, can transactivate endogenous immature intracellular TrkA/B receptors in PC12 cells and hippocampal or cortical neurons (4, 23). Our results show that the catecholamine receptors (D1R and D2R) increase the dimerization of cell surface-expressed EGFR in transfected CHO-k1 cells and TrkB in striatal neurons. These findings indicate that RTK transactivation by dopamine receptors is compatible with normal expression levels of these different receptors and is not restricted to a single cell type. Furthermore, because the D1R and D2R are coupled to G_α and $G_{\alpha i/o}$, it also suggests that TrkB transactivation by GPCR in neurons is not strongly associated with a single type of G-protein coupling and may be compatible with G protein-independent mechanisms involving other signaling molecules like Src and/or β-arrestin (9, 24). It has previously been reported that TrkB transactivation occurs at significantly longer timescales compared with EGFR. Here, we observe that dimerization of TrkB receptors occurs on a similar timescale (3 min) as was observed for EGFR (1 min) when stimulated with Apo, and this dimerization response was similar in magnitude to direct stimulation with BDNF (4). Activation of TrkB by BDNF has been associated with several biological processes, including neuronal survival and neurogenesis, and it is believed to play a role in several neuropsychiatric conditions and/or in the effects of drugs used for their management. Considering the central role of dopamine receptors in the action of drugs used to treat some of these same conditions (25), transactivation of TrkB by dopamine receptors may represent a yet unexplored avenue for the study and management of psychiatric mood disorders and schizophrenia.

We have shown using multiple techniques that quantification of RTK dimerization is a powerful approach to measure transactivation and that this can be applied to studies in native cells. Furthermore, SpIDA is ideally suited for monitoring this process. Indeed, the ability of SpIDA to provide quantitative information on every state of receptor densities, oligomerization state, and localization illuminated the relationship between transactivation and trafficking. These studies revealed that, in most cases, transactivation is directly limited by GPCR activation and expression and that the processes of activation and internalization are not necessarily interdependent, because GPCRs capable of inducing RTK dimerization differ in their ability to induce subsequent internalization. Furthermore, the regulation of RTK activation or internalization by GPCR is not defined by G-protein coupling in transfected cells and intact primary cultured neurons. Finally, by allowing for time and space resolved quantification of heterogeneous oligomeric states, SpIDA makes it possible to undertake quantitative mechanistic studies not only of RTK transactivation at the cell membrane but of other cell-signaling processes involving changes in protein oligomerization, trafficking, and activity in different subcellular localizations.

Methods

Quantitative Analysis of Receptor Dimerization States Using SpIDA. Images used for SpIDA were acquired with conventional Olympus FV300 confocal laser scanning microscopy (CLSM; Olympus) as described (5). Briefly, values obtained from each possible spatial configuration for n particles with quantal brightness ε were weighted by their probability according to a Poisson distribution of particles in space, and the final intensity histogram was calculated. Further details of SpIDA and FLIM/FRET data analysis and experimental procedures are described in *SI Methods*.

ACKNOWLEDGMENTS. We thank Dr. N. Calakos for drd1a-tdTomato transgenic mice, Dr. T. Jovin for the EGFR-GFP cell line, Drs. J. Krause, S. Marion and S. S. Ferguson for Rab5 and GPCR expression vectors, and Dr. P. De Koninck for the monomeric GFP expression vector. J.L.S. and K.D. acknowledge fellowships from the Natural Sciences and Engineering Research Council (NSERC) (Canada). A.G.G. was supported by the Canadian Institutes of Health Research (CIHR) *Neurophysics* Training Program. Y.D.K. is a *Chercheur national* of the Fonds de la Recherche en Santé du Québec (FRSQ). J.-M.B. holds a Canada Research Chair in Molecular Psychiatry. This work was supported by NSERC discovery grants to Y.D.K., P.W.W., and J.-M.B. and a CIHR operating grant to J.-M.B.

1. Lemmon MA, Schlessinger J (2010) Cell signaling by receptor tyrosine kinases. *Cell* 141:1117–1134.
2. Maudsley S, et al. (2000) The beta(2)-adrenergic receptor mediates extracellular signal-regulated kinase activation via assembly of a multi-receptor complex with the epidermal growth factor receptor. *J Biol Chem* 275:9572–9580.
3. Eguchi S, et al. (1998) Calcium-dependent epidermal growth factor receptor transactivation mediates the angiotensin II-induced mitogen-activated protein kinase activation in vascular smooth muscle cells. *J Biol Chem* 273:8890–8896.
4. Rajagopal R, Chen ZY, Lee FS, Chao MV (2004) Transactivation of Trk neurotrophin receptors by G-protein-coupled receptor ligands occurs on intracellular membranes. *J Neurosci* 24:6650–6658.
5. Godin AG, et al. (2011) Revealing protein oligomerization and densities in situ using spatial intensity distribution analysis. *Proc Natl Acad Sci USA* 108:7010–7015.
6. Barbieri MA, et al. (2000) Epidermal growth factor and membrane trafficking. EGF receptor activation of endocytosis requires Rab5a. *J Cell Biol* 151:539–550.
7. Frank GD, Eguchi S, Inagami T, Motley ED (2001) N-acetylcysteine inhibits angiotensin ii-mediated activation of extracellular signal-regulated kinase and epidermal growth factor receptor. *Biochem Biophys Res Commun* 280:1116–1119.
8. Bader AN, Hofman EG, Voortman J, en Henegouwen PM, Gerritsen HC (2009) Homo-FRET imaging enables quantification of protein cluster sizes with subcellular resolution. *Biophys J* 97:2613–2622.
9. Rajagopal S, Rajagopal K, Lefkowitz RJ (2010) Teaching old receptors new tricks: Biasing seven-transmembrane receptors. *Nat Rev Drug Discov* 9:373–386.
10. Zhang ZW, Burke MW, Calakos N, Beaulieu JM, Vaucher E (2010) Confocal analysis of cholinergic and dopaminergic inputs onto pyramidal cells in the prefrontal cortex of rodents. *Front Neuroanat* 4:21.
11. Shuen JA, Chen M, Gloss B, Calakos N (2008) Drd1a-tdTomato BAC transgenic mice for simultaneous visualization of medium spiny neurons in the direct and indirect pathways of the basal ganglia. *J Neurosci* 28:2681–2685.
12. Magde D, Elson EL, Webb WW (1974) Fluorescence correlation spectroscopy. II. An experimental realization. *Biopolymers* 13:29–61.
13. Kask P, Palo K, Ullmann D, Gall K (1999) Fluorescence-intensity distribution analysis and its application in biomolecular detection technology. *Proc Natl Acad Sci USA* 96:13756–13761.
14. Chen Y, Müller JD, So PTC, Gratton E (1999) The photon counting histogram in fluorescence fluctuation spectroscopy. *Biophys J* 77:553–567.
15. Saffarian S, Li Y, Elson EL, Pike LJ (2007) Oligomerization of the EGF receptor investigated by live cell fluorescence intensity distribution analysis. *Biophys J* 93:1021–1031.
16. Ferguson KM (2008) Structure-based view of epidermal growth factor receptor regulation. *Annu Rev Biophys* 37:353–373.
17. Chung I, et al. (2010) Spatial control of EGF receptor activation by reversible dimerization on living cells. *Nature* 464:783–787.
18. Daub H, Weiss FU, Wallasch C, Ullrich A (1996) Role of transactivation of the EGF receptor in signalling by G-protein-coupled receptors. *Nature* 379:557–560.
19. Rantamäki T, et al. (2007) Pharmacologically diverse antidepressants rapidly activate brain-derived neurotrophic factor receptor TrkB and induce phospholipase-Cgamma signaling pathways in mouse brain. *Neuropsychopharmacology* 32:2152–2162.
20. Oakley RH, Laporte SA, Holt JA, Caron MG, Barak LS (2000) Differential affinities of visual arrestin, beta arrestin1, and beta arrestin2 for G protein-coupled receptors delineate two major classes of receptors. *J Biol Chem* 275:17201–17210.
21. Pierce KL, Maudsley S, Daaka Y, Luttrell LM, Lefkowitz RJ (2000) Role of endocytosis in the activation of the extracellular signal-regulated kinase cascade by sequestering and nonsequestering G protein-coupled receptors. *Proc Natl Acad Sci USA* 97:1489–1494.
22. Seachrist JL, Anborgh PH, Ferguson SS (2000) beta 2-adrenergic receptor internalization, endosomal sorting, and plasma membrane recycling are regulated by rab GTPases. *J Biol Chem* 275:27221–27228.
23. Lee FS, Rajagopal R, Kim AH, Chang PC, Chao MV (2002) Activation of Trk neurotrophin receptor signaling by pituitary adenylate cyclase-activating polypeptides. *J Biol Chem* 277:9096–9102.
24. Beaulieu JM, Caron MG (2005) Beta-arrestin goes nuclear. *Cell* 123:755–757.
25. Beaulieu JM, Gainetdinov RR (2011) The physiology, signaling, and pharmacology of dopamine receptors. *Pharmacol Rev* 63:182–217.